Research Article

Journal of PeptideScience

Received: 12 February 2013 Revised: 27 May 2013 Accepted: 19 June 2013 Published online in Wiley Online Library: 25 July 2013

(wileyonlinelibrary.com) DOI 10.1002/psc.2540

Design of NK-2-derived peptides with improved activity against equine sarcoid cells

Stephanie Gross,[a] Dominik Wilms,[b] Jannike Krause,[a] Gerald Brezesinski[c] and Jörg Andrä[a,b]*

Equine sarcoid is a topically accessible model for the evaluation of anticancer peptides acting by physical membrane disruption avoiding the complexity of a systemic application. We aim at evaluating and improving natural peptides for host defence as lead structures, where we focus on the cationic and amphipathic peptide NK-2. Cytotoxicity tests, fluorescence microscopy and a chip-based biosensor, which enabled real-time monitoring of cell metabolism, were applied. Cancer cell killing was dynamic with an initial phase of increased cellular respiration, followed by membrane destruction. NK-2 was substantially improved and shortened. Novel peptides exhibited a fivefold improved activity against sarcoid cells, while haemolysis remained almost unaltered. Similar Zeta potential and similar amount of surface phosphatidylserine of sarcoid and normal skin cells are responsible for a lack of selectivity between these two cell types. Copyright © 2013 European Peptide Society and John Wiley & Sons, Ltd.

Keywords: antimicrobial peptide; skin cancer; phosphatidylserine; membrane; pore formation; Zeta potential

Introduction

Most of the commonly used chemotherapeutics for the treatment of cancer are also harmful to healthy human cells. The used agents are of little or no specificity, so that severe side effects accompany the treatment due to drug-induced damage to healthy cells and tissue. Additionally, cancer cells show an increasing development of resistance mechanisms to formerly effective therapeutics. As a promising alternative, some antimicrobial peptides have been emerged as potential anticancer agents [1–4], which actually exhibit selectivity for cancer cells over healthy, normal cells [5–9]. In contrast to chemotherapeutics, they act primarily by a fast physical disruption of the cancer cell membrane [6,8,10], even though other mechanisms have been suggested [11,12]. Antimicrobial peptides, also called host defence peptides, are widespread in nature occurring in all living organisms such as fungi, plants, animals and humans. They are part of the innate immune system as a first defence line against invading pathogens [13,14]. Selective targeting to microorganisms is based upon an electrostatic interaction of the cationic peptides with the anionic bacterial membrane phospholipids phosphatidylglycerol and cardiolipin [15–17], and lipopolysaccharides [18,19]. However, the molecular basis for selective targeting of these cationic and amphipathic peptides to cancer cells is still controversially discussed. We aim at designing improved anticancer peptides based on natural lead structures, as well as identifying their molecular target structures on cancer cells. Among those targets are negatively charged phospholipids such as phosphatidylserine (PS) [6,20–22] as well as anionic carbohydrates, such as sialic acids [23,24] and sulfated glycans [25–28].

As a cancer model system, we exploited a pair of equine cell lines: sarcoid cells (E42/02) and normal skin cells (APH-R). Skin cancer is an appropriate model for a topical application of peptides avoiding complexities, which come along with a systemic treatment. Actually, equine sarcoid is the most frequently observed skin tumour in horses. It is a locally, invasively growing fibroblastic tumour of the skin with a variable epithelial fraction, which occurs single or multiple, but does not metastasise. Even if it is often just a matter of aesthetics, an equine sarcoid can cause serious problems depending on the location of the tumour and/or its degree of inflammation. A persistently successful treatment of equine sarcoids is very challenging due to a very high relapse rate especially after surgical intervention [29,30]. The recurrence itself is often worse than the original tumour, characterised by growing faster and bigger and with a higher invasive potential [31].

As a lead structure for further improvement and investigation, we focused on the porcine NK-lysin-derived peptide NK-2. In addition, a shortened variant of NK-2, termed NK11, was used as a nontoxic control peptide [28,32]. Melittin, the major lytic component of bee venom, was included as a well-known reference peptide [33]. Our lead peptide NK-2 consists of 27 amino acid residues with an overall positive net charge of +10 and adopts an amphipathic, α-helical secondary structure upon membrane interaction [34,35]. It exhibits activity against Gram-negative and Gram-positive bacteria [17], neutralises bacterial endotoxin [36]

* *Correspondence to: Jörg Andrä, Hamburg University of Applied Science, Faculty of Life Science, Department of Biotechnology, Lohbrügger Kirchstr. 65, D-21033 Hamburg, Germany. E-mail: joerg.andrae@haw-hamburg.de*

a *Division of Biophysics, Research Center Borstel, Leibniz-Center for Medicine and Biosciences, D-23845 Borstel, Germany*

b *Department of Biotechnology, Hamburg University of Applied Science, Lohbrügger Kirchstr. 65, D-21033 Hamburg, Germany*

c *Max Planck Institute of Colloids and Interfaces, Research Campus Potsdam-Golm, 14476 Potsdam, Germany*

Abbreviations used: *MTT*, 3-[4,5-dimethylthiazol-2-yl]-2,5-diphenyltetrazolium bromide; *PS*, phosphatidylserine; *Rh*, rhodamine; *TFE*, trifluoroethanol

and has a proven anticancer cell activity against neuroblastoma [6,32], leukaemia [6] and prostate cancer cells [28]. In contrast, HaCaT cells, i.e. spontaneously transformed human keratinocytes, were less sensitive [32], haemolysis of primary human erythrocytes was low [32] and primary lymphocytes were actually refractory [6].

Materials and Methods

Equine Cell Lines

Equine cell lines used for the given experimental series comprised fibroblast-like normal skin cells (APH-R, CCLV-RIE 958 [37]), as well as sarcoid tumour cells (E42/02, CCLV-RIE 891). Both cell lines were supplied by the Collection of Cell Lines in Veterinary Medicine (CCLV) of the Federal Research Institute for Animal Health (Bundesforschungsinstitut für Tiergesundheit), Greifswald, Insel Riems, Germany. Cells were cultivated in Dulbecco's modified Eagle's medium (Biochrom, Berlin, Germany) supplemented with 10% of heat-inactivated foetal calf serum, 2 mM L-glutamine (Biochrom), 100 U/ml penicillin (Biochrom) and 100 µg/ml streptomycin (Biochrom) at 37 °C in a humidified atmosphere at 5% CO_2. Dependent on the assays used, cell harvest was performed by addition of 1 ml of trypsin/EDTA (Biochrom), accutase (PAA Laboratories GmbH, Pasching, Austria) or enzyme-free cell dissociation buffer (Gibco, Life Technologies, Darmstadt, Germany) and gentle shaking at 37 °C.

Synthetic Peptides

All peptides were synthesised with an amidated C-terminus by the Fmoc solid-phase peptide synthesis technique on an automatic peptide synthesiser (model 433 A: Applied Biosystems) and purified by HPLC as described [38]. The synthesis of rhodamine-labelled peptides (Rh-NK-2 and Rh-NK11) was described earlier in detail [28]. Peptide stock solutions (1 mM) were prepared by solubilisation of the purified and lyophilised peptides in 0.01% TFA and were stored at −20 °C. For peptide sequences, please refer to Table 1.

CD Spectroscopy

CD data were acquired with a Jasco J-715 CD spectrophotometer as described earlier [17]. Spectra were collected for samples of 63 µM peptide in 10 mM phosphate buffer, pH 7.0, in TFE and in the presence of liposomes composed of synthetic 1-palmitoyl-2-oleoyl-phosphatidylserine (1 mM, Avanti Polar Lipids, Alabaster, AL, USA) prepared by the extrusion technique [17]. The secondary structure content was estimated with the help of the DICHROWEB [39,40], using the CONTIN/LL algorithm [41,42].

Fluorescence Microscopy

For confocal fluorescence microscopy of living cells, cells were seeded in culture medium in μ-Slides VI 0.4 (Ibidi, Martinsried, Germany) at a density of 4.8×10^4 cells/well and allowed to attach at 37 °C for 24 h. Cells were washed with PBS and incubated unfixed in the presence of 5 µM sytox green as well as Rh-labelled peptides at room temperature and imaged at indicated time points. Samples were analysed by confocal laser scanning microscopy (TCS SP5, Leica Microsystems, Heidelberg, Germany). All images were acquired using identical settings with Leica LAS AF software.

Cytotoxicity Tests

MTT assay

Cells were harvested by trypsin/EDTA treatment, counted and suspended in complete cell culture medium. This cell suspension (100 µl, 2.5×10^4 cells) was given in each well of a sterile flat bottom 96-well microtitre plate (Costar tissue culture treated, Corning Incorporated, NY, USA) and incubated for 24 h at 37 °C in a humidified atmosphere with 5% CO_2. Peptides from stock solutions were diluted either in complete cell culture medium or in PBS supplemented with 10% of complete cell culture medium (peptide concentrations in each test: 0.1, 0.3, 1, 3, 10, 30 and 100 µM). The respective peptide solution (100 µl) was added to wells of the microtitre plate immediately after the medium has been removed. The plates were then incubated for indicated time at 37 °C in a humidified atmosphere and 5% CO_2. After incubation, 10 µl of a solution (5 mg/ml) of the tetrazolium salt 3-[4, 5-dimethylthiazol-2-yl]-2,5-diphenyltetrazolium bromide (MTT) in PBS, pH 7.4, was added to each well, followed by another incubation period of 2 h at 37 °C. MTT is converted into blue formazan crystals by viable cells. Thus, the change in colour is a measure for the viability of the cells. The reaction was stopped and formazan crystals were dissolved by adding 100 µl of 10% triton X-100 in acid isopropanol to each well. Extinction (M_{Exp}) was measured using a microtitre plate reader (Tecan Rainbow, Crailsheim, Germany) at absorbance and reference wavelengths of 570 and 690 nm, respectively. All experiments were carried out in duplicates

Table 1. Amino acid sequences and modifications of NK-2-derived synthetic peptides used in this study

Peptide	Sequence[a]	Net charge[b]	Remarks
NK-2	KILRGVCKKIMRTFLRRISKDILTGKK	+10	Lead structure, residues 39–65 of porcine NK-lysin [34]
C7A	KILRGV**A**KKIMRTFLRRISKDILTGKK	+10	Cys/Ala substitution ➔ improvement of refractiveness against oxidation
C7A-D21K	KILRGV**A**KKIMRTFLRRISK**K**ILTGKK	+12	Cys/Ala substitution ➔ improvement of refractiveness against oxidation Asp/Lys substitution ➔ enhanced positive net charge (+2)
C7A-Δ	KILRGV**A**KKIMRTFLRR ILTGKK	+10	Cys/Ala substitution ➔ improvement of refractiveness against oxidation deletion of 4 residues ➔ shortening of the peptide
NK11	KISKRILTGKK	+6	NK-2-derived inactive control peptide
Melittin	GIGAVLKVLTTGLPALISWIKRKRQQ	+6	Natural component of bee venom, served as a reference peptide [33]

[a]All peptides were synthesised with an amidated C-terminus.

[b]The net charge of the peptides was calculated by subtracting the number of Asp residues (the only negatively charged amino acid residues present in the peptides) from all the positive charges (Lys, Arg and the peptide's N-terminus). Because the C-terminus of all peptides used was amidated, it did not bear a negative charge.

and performed at least twice. Cells incubated under the respective buffer/medium conditions alone (M_{100}) or in 5% triton X-100 in PBS (M_0) served as positive and negative controls, respectively. Residual metabolic activity (%M) of the cells was calculated using the following equation: $\%M = 100 \times ((M_{Exp} - M_0)/(M_{100} - M_0))$. IC_{50} values indicate that at this peptide concentration, the metabolic activity of the cells was reduced by 50%. These values were derived from the previously described titration curves by sigmoidal fitting.

Propidium iodide-uptake assay

Uptake of the membrane-impermeable DNA-intercalating fluorescent dye propidium iodide is a measure of cell membrane permeabilisation. Cells were harvested by accutase treatment, washed twice with PBS, pH 7.4, adjusted to 2×10^5 cells/ml and sedimented. The supernatant was removed, and peptides (100 µl) diluted in PBS were added to the cell pellet (2×10^5). The suspension was gently vortexed and incubated for 30 min at 37 °C. Subsequently, propidium iodide (5 µl, 100 µg/ml, Invitrogen, Eugene, Oregon, USA) was added, and the cells were incubated for 5 min at 4 °C in the dark. The reaction mixtures were diluted in 900 µl ice-cold PBS and analysed with a FACSCalibur (Becton Dickinson, Heidelberg, Germany) flow cytometer with computer-assisted evaluation of data (CellQuest software). Cell lysis (%L) was calculated from the percentage of dye positive cells in buffer alone (PI_b) and in the presence of peptides (PI_{exp}): $\%L = 100 \times ((PI_{exp} - PI_b)/(100 - PI_b))$. IC_{50} values indicate that at this peptide concentration, fluorescence of the cells reached 50% of the maximal value. These values were derived from the previously described titration curves.

Online monitoring of cell metabolism

For the real-time monitoring of peptide-induced modulation of cell metabolism, we used the Bionas analysing system 1500[2] (Bionas GmbH, Rostock, Germany) essentially as described recently [32]. The system encloses two biomodules, each including one metabolic biosensor chip (SC1000, Bionas), which has three different types of electrodes to measure medium oxygen concentration (Clark), acidification (ion-sensitive field effect transistor), as well as cell layer impedance (interdigitated electrode structure). The system was operated with low buffered running medium to allow the assessment of changes in pH. This running medium is a cell culture medium without bicarbonate buffer but with 1 mM HEPES, pH 7.4, 4.5 g/l glucose, 0.1% foetal calf serum, 100 U/ml penicillin and 100 µg/ml streptomycin (Bionas GmbH). Cells harvested by trypsin/EDTA treatment were immobilised in agarose on a membrane disc and placed in the chips (4×10^5 cells). Agarose embedding of cells was necessary because the used equine cells did not grow with a sufficient adherence on the chips. Embedding was performed using the Bionas kit for cell suspensions following the instructions of the manufacturer (Bionas GmbH). As a consequence, the opportunity for measuring changes in cell morphology (interdigitated electrode structure sensor) was forfeited. Briefly, one volume of melted agarose ready-to-use solution was mixed with two volumes of a cell suspension in medium (6×10^7 cells/ml). This agarose–cell mixture (10 µl) was dropped on a sterile membrane disc (4×10^5 cells/membrane). The membrane disc with the hardened agarose–cell drop was placed upside down into a sensor chip filled with medium. In the course of an experiment, all chips were initially flushed with running medium for 4 h, followed by a 12 h feed of either running medium (as a control) or peptides in running medium. After that, a 4-h perfusion with running medium is carried out to allow recovery of cells. At the end of each experiment, biomodules were rinsed with 0.2% triton X-100 in running medium to achieve complete cell lysis. We used a flow rate of 56 µl/min with alternating 'go' and 'stop' phases of 4 min each. During the go phase, cells on the chip are perfused with fresh medium or medium with compound. In the subsequent stop phase, flow was stopped, and oxygen consumption and extracellular acidification of the cell supernatant on each chip were measured continuously. The change of the parameters during the stop phase was calculated and is given as a single data point in the figures. Presented data are the mean of two independent cell preparations.

Assay for haemolytic activity

Freshly isolated and washed human erythrocytes (5×10^8 cells/ml) in 20 µl PBS, pH 7.4, were incubated with 80 µl of a peptide sample in the same buffer for 30 min at 37 °C in a round bottom 96-well plate (Nunclon Surface, Nunc, Roskilde, Denmark). After the incubation period, the plate was centrifuged at 1000 *g* for 10 min to remove intact erythrocytes, and the concentration of released haemoglobin was measured in a microtitre plate reader at 405 nm (Rainbow, Tecan, Grödig/Salzburg, Austria) after tenfold dilution of the supernatant. Haemolytic activity was expressed as percent haemolysis ($\%\text{haemolysis} = ((OD_{Sample} - OD_{buffer})/(OD_{max} - OD_{buffer})x100)$). Maximal lysis ($OD_{max}$) was achieved by adding distilled water instead of the peptide sample to the cells. Data shown represent the mean of at least four experiments each performed in duplicate.

Determination of PS Exposed on the Cell Surface

The content of negatively charged PS in the outer membrane leaflet of cells was determined by measuring the amount of binding of fluorescently labelled annexin V as well as of a PS-specific antibody to the cells. Cells were harvested by accutase treatment, washed twice with PBS, pH 7.4, and sedimented. After incubation with the respective reagents (see succeeding text), cell suspensions were analysed with a FACSCalibur (Becton Dickinson, Heidelberg, Germany) flow cytometer with computer-assisted evaluation of data (CellQuest software, Becton Dickinson).

Annexin V

Fluorescein isothiocyanate-labelled annexin V (100 µl, Biolegend, San Diego, CA, USA), 1% in binding buffer (10 mM HEPES, 150 mM NaCl, 5 mM KCl, 1 mM $MgCl_2$, 1.8 mM $CaCl_2$, pH 7.4), was added to the cell pellet (2×10^5), and the suspension was gently vortexed and incubated for 15 min in the dark. Subsequently, 400 µl ice-cold binding buffer was added, and the suspension was kept on ice until being analysed.

PS-specific antibody

A PS-specific monoclonal antibody (100 µl, 0.5 µg/ml, mouse monoclonal [4B6], Abcam, Cambridge, UK) was added to the cell pellet (2×10^5). The suspension was gently vortexed and incubated for 1 h in the dark. Subsequently, the cells were washed once again with PBS and resuspended with Alexa 647-labelled goat anti-mouse IgG (H + L, Alexa Fluor® 647, Molecular Probes, Carlsbad, CA, USA) in PBS (100 µl, 1 : 1000) and incubated for 30 min in the dark. After another washing cycle, the cells were diluted in 1 ml PBS and kept on ice until being analysed.

Determination of Zeta Potential of Cells

Cells were harvested by treatment with enzyme-free cell dissociation buffer (Gibco, Life Technologies), filtered through gaze (TG100, Schleicher und Schuell, Dassel, Germany) and adjusted to 10^6 cells/ml in 40 mM HEPES, pH 7.4. For Zeta potential measurements, 200 µl of cell suspension was diluted in 800 µl buffer and placed in a sample cell (Malvern Instruments GmbH, Herrsching, Germany). Measurements were performed using a ZetaSizer NanoSeries (Malvern). The velocity (v) of cells in a driving electric field (E) of an effective voltage of 152 V was measured by dynamic light scattering, and the corresponding electrophoretic mobilities (v/E) were calculated. The associated Zeta potentials were calculated by the Smulochowski approximation. Six measurements were performed and averaged for each sample. Data presented are the mean of two independent cell preparations.

Results

NK-2 is Active Against Equine Sarcoid Cells

In a first set of experiments, we characterised the anticancer cell activity of peptide NK-2 and of two reference peptides (NK11 and melittin) against equine sarcoid cells (E42/02) and normal, fibroblast-like equine skin cells (APH-R) using two distinct buffer conditions. NK11 is an 11-residue derivative of NK-2 and served as an inactive control peptide [28]. Melittin was included in this and the following assays as a reference peptide. It is a cationic linear α-helical peptide from bee venom, well known for its potent haemolytic and antibacterial activities [33]. The peptides were added to the cells seeded on microtitre plates either in PBS supplemented with 10% medium or in medium. After 4 h, the residual metabolic activity of the cells was determined by the MTT test. The assay results are shown exemplarily for E42/02 cells in detail (Figure 1) and are summarised in Tables 2 and 3. NK-2 exhibited potent activity in buffer supplemented with medium (Figure 1, Table 2); however, activity drastically dropped in complete medium (Table 3). Melittin was more or less unaffected by incubation conditions, and as expected, NK11 had no cytotoxicity. Both, NK-2 and melittin, exhibited no selectivity for E42/02 over APH-R cells.

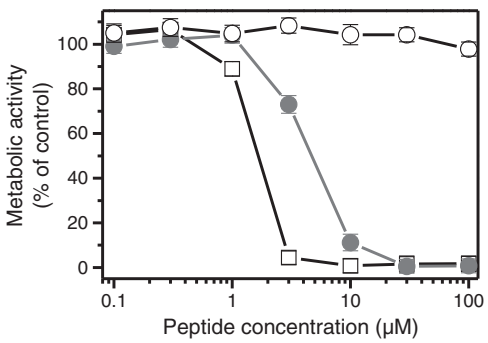

Figure 1. Anticancer cell activity of peptides. Metabolic activity of E42/02 sarcoid cells measured by the MTT assay in PBS supplemented with 10% medium. Cells were incubated in the buffer/medium mix as a control or with peptides (NK-2, grey circles; NK11, open circles; melittin, open squares) at indicated concentrations for 4 h at 37 °C.

Table 2. Cytotoxicity of peptides NK-2, NK11 and melittin

	PBS with 10% medium	
Peptide	E42/02 IC_{50} (µM)	APH-R IC_{50} (µM)
NK-2	4.3 ± 0.3	3.2 ± 0.2
NK11	>>100	>>100
Melittin	1.4 ± 0.1	0.9 ± 0.1

Cytotoxicity of peptides against equine cells E42/02 and normal skin cells APH-R was determined by the MTT assay after 4 h incubation at 37 °C in PBS supplemented with 10% medium. Given are IC_{50} values (in µM) at which the viability of the cells was reduced by 50%.

Table 3. Time dependence of peptide-induced cell killing; activities are given as IC_{50} in µM

Peptide	30 min	2 h	4 h	24 h
E42/02 in 100% medium				
NK-2	≈70	≈50	≈50	≈40
C7A	10.6 ± 0.4	13.0 ± 1.0	12.1 ± 1.6	37 ± 4.3
C7A-D21K	8.4 ± 0.2	12.3 ± 2.0	8.3 ± 0.5	12.3 ± 1.0
C7A-Δ	7.5 ± 0.4	13.8 ± 2.0	9.3 ± 1.5	13.1 ± 0.9
NK11	>>100	>>100	>>100	>>100
Melittin	3.2 ± 0.1	2.1 ± 0.1	1.8 ± 0.1	1.4 ± 0.1
APH-R in100% medium				
NK-2	≈70	≈60	≈50	≈45
C7A	8.9 ± 0.3	11.1 ± 0.3	11.8 ± 1.2	15.0 ± 2.4
C7A-D21K	6.9 ± 0.5	10.9 ± 0.6	10.7 ± 1.0	13.1 ± 1.2
C7A-Δ	6.2 ± 0.2	9.8 ± 0.7	9.4 ± 1.2	12.4 ± 0.9
NK11	>>100	>>100	>>100	>>100
Melittin	3.2 ± 0.1	2.6 ± 0.1	2.2 ± 0.1	1.3 ± 0.1

Viability of equine sarcoid (E42/02, upper table) and skin cells (APH-R, lower table) was assessed in complete medium by the metabolic MTT test after indicated incubation times at 37 °C. Given are peptide concentrations at which the viability of cells was reduced by 50% (IC_{50} in µM). These values were derived from titration curves by sigmoidal fitting (except for NK-2 and NK11).

Fluorescence Microscopic Analysis of NK-2-induced Killing of E42/02 Cells

Cells were seeded on microscopic slides and monitored in an unfixed, viable state, in the presence of various concentrations of NK-2 and NK11 labelled with the fluorophore rhodamine (Rh-NK-2 and Rh-NK11) and the membrane-impermeable DNA-intercalating fluorescent dye sytox green. Upon addition of 1 µM Rh-NK-2 (Figure 2D–F), a pale red seam was observed at the cells after a few minutes. Single cells became sytox green positive, thereby indicating cell killing by membrane permeabilisation. The number of dead cells did not increase significantly after long-term incubation (up to 60 min). At 3 µM Rh-NK-2 (Figure 2G–I), a red seam was observed at the cells immediately after addition of the peptide. After a few minutes, first, cells were permeabilised, and after 30 min approximately, 70% of cells were sytox green positive. The peptide also stained intracellular membranes and, like sytox green, traversed the nuclear membrane (bright yellow fluorescence). In addition, large bubbles, only stained red at the rim, were visible in the cytosol. Upon addition of 5 µM Rh-NK-2 (Figure 2J–L), single cells were permeabilised within 1 min, and almost all cells were dead within minutes. Most cells showed massive bleb formation. In contrast to

Journal of PeptideScience

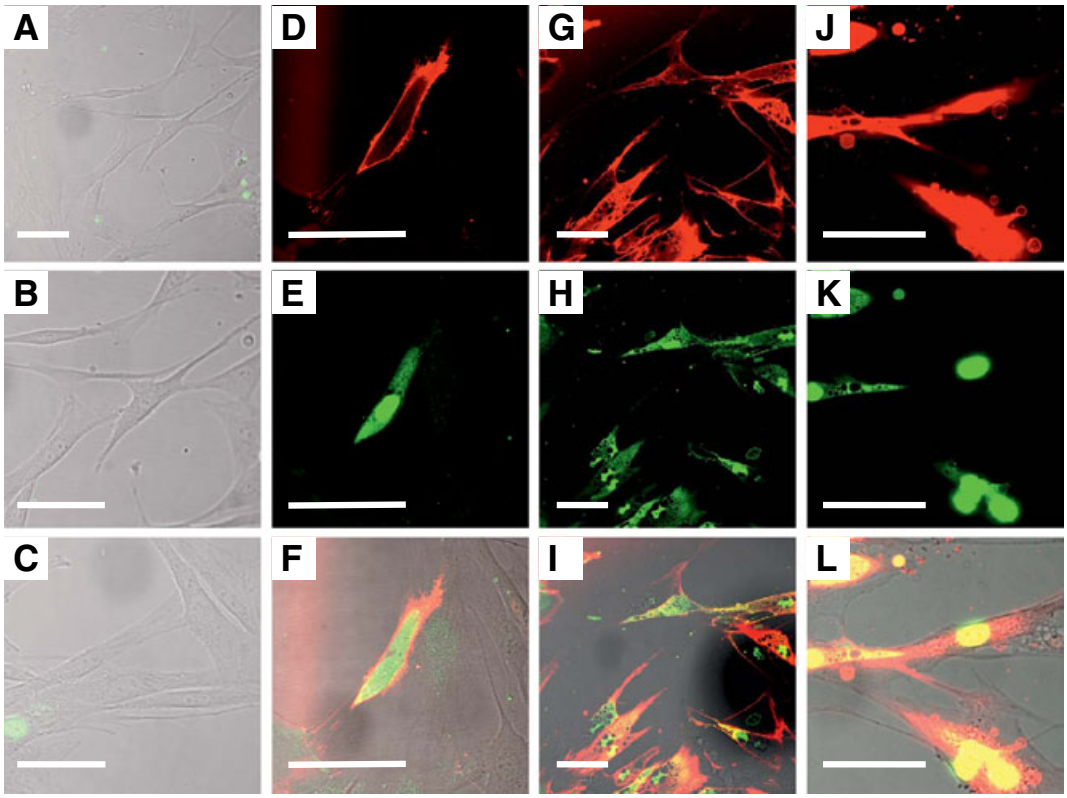

Figure 2. NK-2 binding to E42/02 cells and subsequent cell lysis. NK-2-induced binding and cell membrane permeabilisation of E42/02 cells were visualised by confocal fluorescence microscopy. Cells were incubated in buffer with membrane-impermeable dye sytox green (green fluorescence) and three concentrations of Rh-NK-2 (red fluorescence). (D–F) 1 μM for 13 min; (G–I) 3 μM for 6 min; (J–L) 5 μM for 6 min. Red and green channels are presented in the upper (D, G, J) and middle row (E, H, K), respectively. Bottom row (F, I, L) represents an overlay of brightfield, green and red channels. Untreated (control) cells (A, B, C) are shown as an overlay of brightfield and green fluorescence. Scale bar = 50 μm.

NK-2, the noncytotoxic peptide NK11 only exhibited a marginal binding to the cell surface, which was expressed in a scarcely apparent red stain (not shown). Cellular morphology was indistinguishable to control cells.

Design of (Improved) NK-2 Variants

We synthesised three new variants of NK-2 to enhance stability, positive net charge, as well as to shorten the parent peptide (Table 1). The most basic modification entailed the replacement of the nonfunctional sole Cys^7 residue within the NK-2 sequence with an Ala residue (C7A). This substitution did not clearly change the structural properties of NK-2 (Table 4), whereas it is expected to reduce the sensitivity of the peptides to oxidation, thereby improving stability. Both peptides were found to be mainly unstructured in phosphate buffer, whereas they adopted a primarily α-helical secondary structure in a hydrophobic environment such as TFE as well as in the presence of negatively charged lipid vesicles composed of PS (Figure 3). An enhancement of C7A's positive net charge was achieved by substituting Asp^{21} by a Lys residue (C7A-D21K). Moreover, we shortened C7A by deletion of a stretch of four amino acid residues (including Asp^{21}), resulting in peptide C7A-Δ.

Table 4. Secondary structure elements of peptides NK-2 and C7A

Peptide	Helix (%)	Strand (%)	Turn (%)	Unordered (%)
NK-2				
Buffer	8	34	23	34
TFE	56	11	16	26
PS	48	15	15	20
C7A				
Buffer	8	30	23	37
TFE	62	3	15	19
PS	49	20	9	20

Secondary structure elements of peptides were determined by CD spectroscopy in phosphate buffer (buffer), TFE, and in the presence of negatively charged lipid vesicles made of phosphatidylserine (PS).

Comparative Cytotoxic Activity of NK-2 and Derived Peptides Against Equine Cell Lines

The cytotoxic effects of NK-2, control peptides, as well as of the newly synthesised peptides, were investigated against E42/02 and APH-R cells using three different assays: (i) the MTT test was performed to determine the residual metabolic activity of the cells; (ii) a chip-based sensor was used to monitor the effects of peptides on the metabolic activity of the cells in real time; and finally, (iii) peptide-induced membrane damage was assessed by a dye-uptake assay.

Time course of cytotoxicity of NK-2 and of newly designed analogues

Cells in complete medium were incubated from 30 min to 24 h in the presence of various amounts of peptides. After the incubation period, the residual viability of cells was determined by the

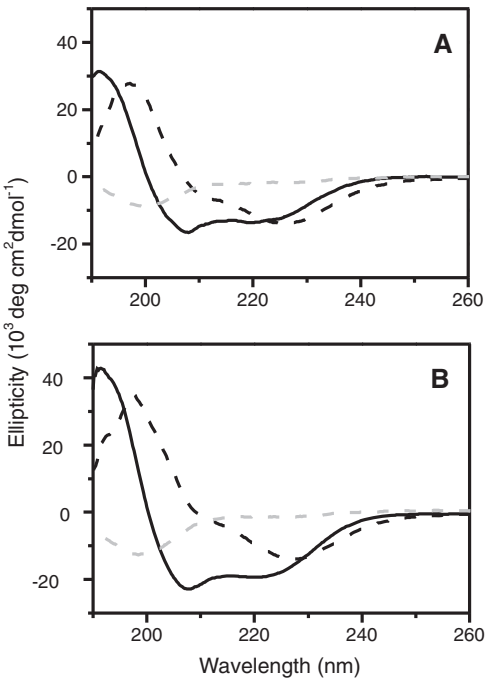

Figure 3. Secondary structures of NK-2 and C7A. CD spectroscopy for (A) NK-2 and (B) C7A in buffer (grey dashed line), in TFE (solid line) and in the presence of PS liposomes (black dashed line). Data for NK-2 in buffer and TFE were taken from [17].

MTT test (Table 3). NK-2 exhibited rather low potency, which, however, slightly increased over time. Any of the modifications substantially improved peptide NK-2. Actually, the Cys/Ala exchange was the key substitution. This exchange did not alter the net charge but improved the IC_{50} value of NK-2 by a factor of 4–7. Substitution or deletion of the negatively charged Asp residue further led to a slight improvement in activity. Peptide's action on the cells was more or less completed within 30 min. A slight decrease in activity was observed, however, for C7A, C7A-D21K and C7A-Δ between 4 and 24 h. This effect was most pronounced for C7A against E42/02 cells and might indicate adsorption or even slow proteolytic digest of the peptides. Apparently, no selectivity for the sarcoid cells over normal skin cells could be achieved.

Real-time monitoring of peptide-induced changes in cell metabolism

To obtain a deeper insight into the dynamics of peptide–cell interaction, the impact of selected peptides on the cellular rates of respiration and acidification (e.g. the energy metabolism) of E42/02 (Figure 4A) and of APH-R cells (Figure 4B) was monitored in real time and online over 12 h by the use of a chip-based sensor. Peptides were added routinely after a 4-h equilibration phase of the cells with pure medium perfusion. After that time, cells had adapted to the perfusion system, and metabolic rates for cell respiration (changes in O_2 signal) and acidification (changes in pH) remained more or less constant for >20 h (not shown). A decrease of metabolic rates (respiration and acidification) was registered in the event of cell dying. Only negligible effects on the metabolic activity of the two cell lines were observed during perfusion with the parent peptide NK-2. In the presence of the most promising variant C7A-D21K, however, the cells displayed a very interesting behaviour. Both cell lines responded quickly by a steep increase in the respiration rate, indicating an escalated necessity for energy to combat the deleterious effects of the peptide. After this metabolically active phase, rates went down, indicating cell death. No recovery of cells was observed

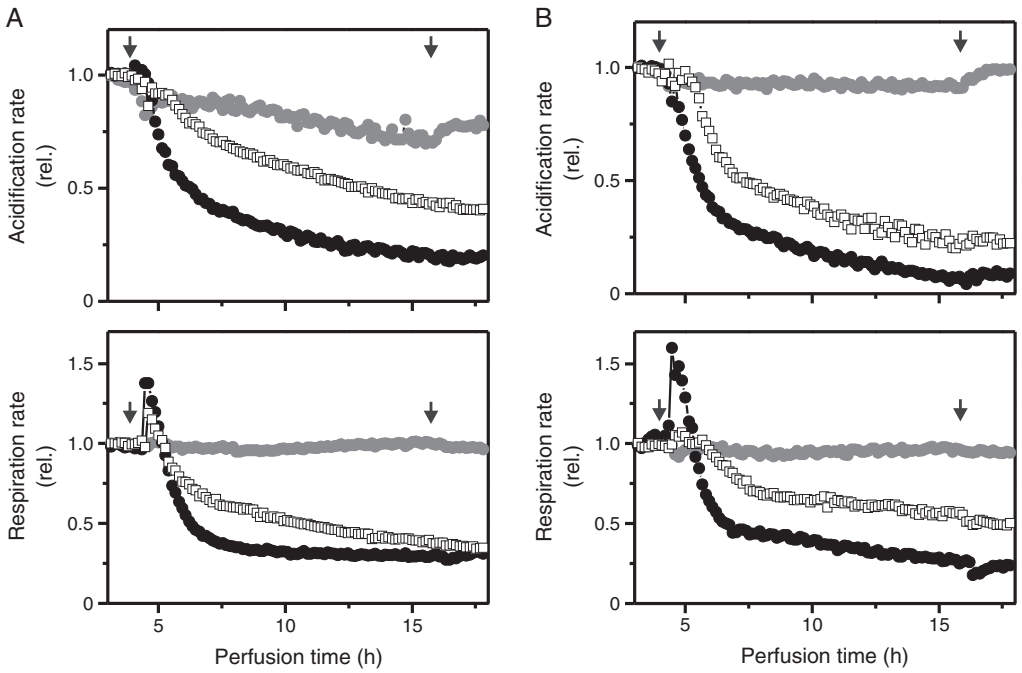

Figure 4. Online monitoring of cell metabolism by the use of a chip-based biosensor. (A) E42/02 cells and (B) APH-R cells were immobilised on a chip and perfused with medium that contained the following peptides: NK-2 (10 μM, grey circles), C7A-D21K (10 μM, black circles) and melittin (3 μM, open squares). Peptide perfusion lasts from 4 to 16 h (arrows). Acidification and respiration rates (oxygen consumption) of peptide-treated cells are shown relative to untreated control cells.

Journal of PeptideScience

when perfusion was continued with pure medium (16 h). Melittin exhibited higher activity and was used here at a lower concentration (3 μM) than the other two peptides (10 μM). Additionally, melittin triggered an enhanced respiration rate. Again, no significant differences between E42/02 and APH-R cells could be observed.

Membrane permeabilisation of equine cells by NK-2 and derivatives

Peptide-induced cell membrane permeabilisation was determined by measuring the uptake of the fluorescent dye propidium iodide by subsequent FACS analysis (Table 5). All peptides permeabilised the cell membrane of both cell types, clearly stating that interaction with the membrane is crucial for cell killing. Moreover, the newly designed NK-2 variants were of greater efficacy than the parent peptide itself. Here, C7A was the most effective peptide, actually beating melittin in killing of E42/02 sarcoid cancer cells. Again, no selectivity for the E42/02 cells was observed. If any, the normal skin cells were even more sensitive than the sarcoid cells.

Haemolytic activity of NK-2 and derivatives

Haemolysis was determined by measuring the release of haemoglobin from freshly isolated human erythrocytes after 30 min incubation with the peptides (Figure 5). As it has been shown earlier, melittin exhibited high, NK-2 moderate and NK11 no haemolytic activity [32]. The enhanced anticancer cell activity of C7A was paralleled by an increased haemolysis compared with NK-2, although still far below melittin. In contrast, C7A-D21K as well as C7A-Δ exhibited a similarly moderate haemolysis as NK-2, although they were highly active against cancer cells.

Table 5. Peptide-induced membrane permeabilisation

Peptide	E42/02 IC_{50} (μM)	APH-R IC_{50} (μM)
NK-2	16.6 ± 0.6	6.6 ± 0.4
C7A	6.8 ± 0.4	5.7 ± 0.7
C7A-D21K	13.7 ± 0.9	4.1 ± 0.3
C7A-Δ	12.6 ± 0.7	8.1 ± 0.3
NK11	>>100	>>100
Melittin	12.7 ± 0.2	5.0 ± 0.4

Peptide-induced membrane permeabilisation of E42/02 and APH-R cells was determined after 30 min incubation at 37 °C by measuring the cellular uptake of the fluorescent dye propidiumiodide. Given are the peptide concentrations (IC_{50} in μM) at which 50% of the cells were dye positive. IC_{50} values were derived from titration curves by sigmoidal fitting.

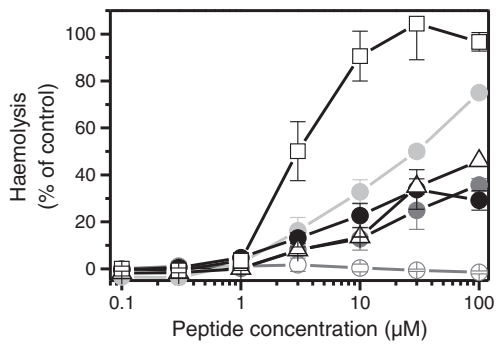

Figure 5. Haemolytic activity of peptides. Lysis of human erythrocytes was determined photometrically by measuring the release of haemoglobin after incubation with the following peptides: NK-2 (grey circles), C7A (light grey circles), C7A-D21K (black circles), C7A-Δ (open triangles), NK11 (open circles) and melittin (open squares).

Analysis of the Cell Surface of Equine E42/02 and of APH-R Cells

The absolute lack of selectivity of the peptides for any of the two equine cell lines prompted us to investigate the portion of negative charges on the cell surfaces. The most prominent target structure for cationic peptides on the cell surface is the anionic phospholipid PS. We determined the relative amount of PS on the cell surface by FACS analysis by binding of a PS-specific antibody and by annexin V binding to the cells and observed no significant differences between APH-R and E42/02 cells (not shown). Thus, we conclude that the E42/02 sarcoid cells have no increased amount of PS on the surface and that both cell lines expose a similar low amount of PS to the exterior.

Moreover, we determined the Zeta potential of the cells. The Zeta potential is the accessible surface charge of a particle, here the cell surface, and thus an important parameter for the interaction with cationic peptides. We obtained negative Zeta potentials of −17.8 ± 0.8 V and of −16.7 ± 1.9 V for E42/02 and APH-R cell suspensions, respectively. Thus, there was no significant difference in Zeta potential between the two cell lines.

Discussion

Optimisation of Peptides

NK-2 is a very effective peptide at low micromolar concentrations against a considerable number of cancer cells including human neuroblastoma, leukaemia, colorectal adenocarcinoma and prostate cancer [6,28,32], non-small cell lung carcinoma [43], as well as equine sarcoid cancer (this study). However, the peptide apparently exhibits reduced efficacy under full medium conditions ([6,32] and in particular this study). To overcome this restriction, we designed three novel peptides based on NK-2 by rational approach. Replacement of Cys^7 residue (peptide C7A) is thought to reduce sensitivity to oxidation. This Cys residue, although it is involved in disulfide bonding in the protein NK-lysin [44], from which NK-2 was derived [34], is nonfunctional in peptide NK-2 itself [17]. Enhancement of the positive net charge has been shown to improve the antibacterial activity of a variety of peptides [17] and seemed also to be relevant for the anticancer activity [45]. Here, we exchanged an anionic Asp^{21} residue by cationic Lys leading to peptide C7A-D21K. Finally, size reduction was achieved by the consecutive omission of a putative internal helical term of the peptide NK-2. This deletion of a consecutive stretch of four amino acid residues, including the anionic Asp^{21} and cationic Lys^{20} residue (leading to peptide C7A-Δ), maintains the amphipathic nature and charge pattern of the parent peptide NK-2. Actually, the Cys/Ala exchange (C7A) turned out to be the key substitution to maintain the peptide's activity also under medium conditions. The reason for that is currently unclear. As discussed earlier [17], we do not believe that peptide dimerisation is involved. Instead, we suggest that an enhanced hydrophobicity of the Ala residues contributes to the behaviour of the peptide.

Substitution or deletion of anionic Asp^{21} further improved activity, in particular in a long-term regime. It is important to note that also the shortened derivative C7A-Δ, implying a significantly reduced synthesis effort, represents a substantially improved version of the anticancer peptide NK-2. The same consecutive deletion of amino acid residues 18–21 (Ile-Ser-Asp-Lys) was already successful in an earlier study, which was devoted to the antibacterial activity of NK-2-derived peptides [17]. These peptides were based upon a Cys/Ser instead of the Cys/Ala exchange used in this study. At this stage, we cannot yet define the molecular basis for the antibacterial and anticancer cell activities of NK-2-derived peptides. Both activities require a positive net charge of the peptides. However, it seems likely that other molecular requirements for these two targets are indeed different. This assumption is stressed by the fact that peptide C7S, which differs from NK-2 by a single substitution of Cys^{7} against Ser, exhibits improved antibacterial activity [17] but inferior activity against cancer cell lines (not shown). Further enhancement of the cationic charge of C7A (net charge +10), leading to peptide C7A-D21K (net charge +12), did not significantly improved activity against equine cancer cells. Importantly, selectivity was not the toll for an improved anticancer cell activity, because the novel peptides exhibited a similar low to moderate haemolytic activity as NK-2.

Mode of Action

Dynamics of the peptide–cell interaction process were monitored in more detail for NK-2 and C7A-D21K using confocal fluorescence microscopy as well as a chip-based sensor for pH and oxygen. Binding of NK-2 to the cell surface was rapid, within seconds, and, above a critical concentration, was followed almost immediately by membrane blebbing and membrane permeabilisation. Subsequently, the peptide enters the cytosol. Obviously, the accumulation dynamics were dependent on the peptide concentration applied and lasted from seconds up to 10 min. After traversing the plasma membrane, NK-2 bound to intracellular membranes, induced the formation of large intracellular bubbles and entered the nucleus in a fast sequence.

The initial binding phase was accompanied by a dramatically increased respiration rate of the cells, which was documented for C7A-D21K using the chip-based sensor. These data go hand in hand with results from the classical MTT test, where the highest effectiveness of the peptides was also found within the first 30 min of incubation. Thus, peptides bind rapidly and permeabilise the membrane, thereby inducing massive cell stress, which leads to membrane blebbing and enhanced energy metabolism in order to repel the peptide's attack. A comparable increase has also been observed also for melittin against HaCaT cells but not for NK-2 against sensitive neuroblastoma cells [32]. We suppose that the reaction of HaCaT and the equine cells to the peptide-induced membrane damage is an indication of a more robust, tenable cell type. Compared with conventional chemotherapeutics, the mode of action of the peptides is extremely fast. Physical membrane destruction, combined with a fast killing process, is likely to be the basis for their capacity to overcome known resistances against current drugs [43,46] and their low tendency for the generation of new resistances.

Cell Type Selectivity

Regrettably, none of the peptides discriminated between equine normal skin fibroblasts and sarcoid cells. This was surprising, because peptide NK-2 exhibited clear selectivity for neuroblastoma cancer cells over HaCaT cells [32], which represent noncancerous, spontaneously transformed human keratinocytes [47]. Meanwhile, it is well accepted that some cancer cells expose an increased amount of the negatively charged membrane lipid PS in the outer leaflet of their plasma membranes, which leads to an increased negative net charge on the surface of those cells [6,20,22], and thus triggers the interaction with the cationic peptides [6,48]. A direct PS interaction has been documented before for NK-2 [6,49] and is also emphasised here by the adoption of an α-helical secondary structure by NK-2 and C7A in the presence of PS liposomes.

Actually, the amount of PS, which was detectable on the surface of the sarcoid and normal skin cells, was undistinguishable. In addition, also other charged surface factors were found to be present in a similar amount/density on the cell surface, as indicated by a similar Zeta potential, a measure of the accessible surface charge. Similar amounts of surface-exposed PS as well as of other potentially anionic structures on both cell lines provide a reasonable explanation for the lack of selectivity of the peptides. Besides PS, anionic carbohydrates, such as terminal sialic acid residues on glycoproteins and glycolipids as well as sulfated glycosaminoglycans, contribute to the Zeta potential of cells. NK-2 and peptides derived thereof apparently prefer binding to PS and sulfated glycans (chondroitin sulfate) rather than to sialic acids (this study and [6,28]). In a recent study, it has been shown that killing of A549 lung carcinoma cells by a model peptide occurs before neutralisation of the Zeta potential of the cells [50]. In the light of our findings, it sounds reasonable that this residual Zeta potential is rested upon unmasked sialic acid residues on the cell surface.

Conclusions

Cationic, amphipathic peptides are potential anticancer drugs with a novel mode of action. Here, we achieved a substantial improvement of peptide NK-2 by directed amino acid substitutions, leading to a more stable, shortened version of the parent peptide (C7A-Δ). Moreover, we documented for the first time an efficacy of a cationic, amphipathic peptide against equine cancer cells, showed that the anticancer activity of NK-2 and of the improved peptides is driven by membrane permeabilisation and gave a reasonable explanation for a similar sensitivity of the sarcoid and normal skin cell lines. Because the peptides were effective against the sarcoid cells *in vitro*, a successful therapeutic approach may combine surgery followed by a local application of peptides directly at the tumour site. All presented peptides also exhibit potent antibacterial activities (unpublished data and [17,51]). Thus, this procedure may minimise the relapse rate by the eradication of remaining sarcoid cells as well as prevent a bacterial wound infection.

Acknowledgements

We would like to give our thanks to Sabrina Groth for the excellent technical assistance in cell culture and FACS analysis, Kerstin Stephan for performing the haemolysis assay, Claudia Olak for the CD measurements, and Rainer Bartels and Volker Grote for the peptide synthesis. This work is part of the doctoral theses of S. G. and of D. W. It was financially supported by the German Research Foundation (Deutsche Forschungsgemeinschaft, DFG, grant AN301/5-1) to J. A.

Journal of PeptideScience

References

1 Leuschner C, Hansel W. Membrane disrupting lytic peptides for cancer treatments. *Curr. Pharm. Des.* 2004; **10**: 2299–2310.
2 Papo N, Shai Y. Host defence peptides as new weapons in cancer treatment. *Cell. Mol. Life Sci.* 2005; **62**: 784–790.
3 Schweizer F. Cationic amphiphilic peptides with cancer-selective toxicity. *Eur. J. Pharmacol.* 2009; **625**: 190–194.
4 Riedl S, Zweytick D, Lohner K. Membrane-active host defense peptides – challenges and perspectives for the development of novel anticancer drugs. *Chem. Phys. Lipids* 2011; **164**: 766–781.
5 Papo N, Shahar M, Eisenbach L, Shai Y. A novel lytic peptide composed of DL-amino acids selectively kills cancer cells in culture and in mice. *J. Biol. Chem.* 2003; **278**: 21018–21023.
6 Schröder-Borm H, Bakalova R, Andrä J. The NK-lysin derived peptide NK-2 preferentially kills cancer cells with increased surface levels of negatively charged phosphatidylserine. *FEBS Lett.* 2005; **579**: 6128–6134.
7 Sand SL, Haug TM, Nissen-Meyer J, Sand O. The bacterial peptide pheromone plantaricin A permeabilizes cancerous, but not normal, rat pituitary cells and differentiates between the outer and inner membrane leaflet. *J. Membr. Biol.* 2007; **216**: 61–71.
8 Wang KR, Yan JX, Zhang BZ, Song JJ, Jia PF, Wang R. Novel mode of action of polybia-MPI, a novel antimicrobial peptide, in multi-drug resistant leukemic cells. *Cancer Lett.* 2009; **278**: 65–72.
9 Chen YQ, Min C, Sang M, Han YY, Ma X, Xue XQ, Zhang SQ. A cationic amphiphilic peptide ABP-CM4 exhibits selective cytotoxicity against leukemia cells. *Peptides* 2010; **31**: 1504–1510.
10 Tang C, Shao X, Sun B, Huang W, Qiu F, Chen Y, Shi YK, Zhang EY, Wang C, Zhao X. Anticancer mechanism of peptide P18 in human leukemia K562 cells. *Org. Biomol. Chem.* 2010; **8**: 984–987.
11 Okumura K, Itoh A, Isogai E, Hirose K, Hosokawa Y, Abiko Y, Shibata T, Hirata M, Isogai H. C-terminal domain of human CAP18 antimicrobial peptide induces apoptosis in oral squamous cell carcinoma SAS-H1 cells. *Cancer Lett.* 2004; **212**: 185–194.
12 Chen J, Xu XM, Underhill CB, Yang S, Wang L, Chen Y, Hong S, Creswell K, Zhang L. Tachyplesin activates the classic complement pathway to kill tumor cells. *Cancer Res.* 2005; **65**: 4614–4622.
13 Zasloff M. Antimicrobial peptides of multicellular organisms. *Nature* 2002; **415**: 389–395.
14 Hancock RE, Sahl HG. Antimicrobial and host-defense peptides as new anti-infective therapeutic strategies. *Nat. Biotechnol.* 2006; **24**: 1551–1557.
15 Matsuzaki K, Sugishita K, Fujii N, Miyajima K. Molecular basis for membrane selectivity of an antimicrobial peptide, magainin 2. *Biochemistry* 1995; **34**: 3423–3429.
16 Schröder-Borm H, Willumeit R, Brandenburg K, Andrä J. Molecular basis for membrane selectivity of NK-2, a potent peptide antibiotic derived from NK-lysin. *Biochim. Biophys. Acta* 2003; **1612**: 164–171.
17 Andrä J, Monreal D, Martinez de Tejada G, Olak C, Brezesinski G, Sanchez Gomez S, Goldmann T, Bartels R, Brandenburg K, Moriyon I. Rationale for the design of shortened derivatives of the NK-lysin derived antimicrobial peptide NK-2 with improved activity against gram-negative pathogens. *J. Biol. Chem.* 2007; **282**: 14719–14728.
18 Gutsmann T, Hagge SO, David A, Roes S, Böhling A, Hammer MU, Seydel U. Lipid-mediated resistance of Gram-negative bacteria against various pore-forming antimicrobial peptides. *J. Endotoxin Res.* 2005; **11**: 167–173.
19 Hammer M, Brauser A, Olak C, Brezesinski G, Goldmann T, Gutsmann T, Andrä J. Lipopolysaccharide interaction is decisive for the activity of the antimicrobial peptide NK-2 against *Escherichia coli* and *Proteus mirabilis*. *Biochem. J.* 2010; **427**: 477–488.
20 Utsugi T, Schroit AJ, Connor J, Bucana CD, Fidler IJ. Elevated expression of phosphatidylserine in the outer membrane leaflet of human tumor cells and recognition by activated human blood monocytes. *Cancer Res.* 1991; **51**: 3062–3066.
21 Ran S, Thorpe PE. Phosphatidylserine is a marker of tumor vasculature and a potential target for cancer imaging and therapy. *Int. J. Radiat. Oncol. Biol. Phys.* 2002; **54**: 1479–1484.
22 Riedl S, Rinner B, Asslaber M, Schaider H, Walzer S, Novak A, Lohner K, Zweytick D. In search of a novel target — phosphatidylserine exposed by non-apoptotic tumor cells and metastases of malignancies with poor treatment efficacy. *Biochim. Biophys. Acta* **2011**; 1808: 2638–2645.
23 Miyagi T, Wada T, Yamaguchi K, Shiozaki K, Sato I, Kakugawa Y, Yamanami H, Fujiya T. Human sialidase as a cancer marker. *Proteomics* 2008; **8**: 3303–3311.
24 Weghuber J, Aichinger MC, Brameshuber M, Wieser S, Ruprecht V, Plochberger B, Madl J, Horner A, Reipert S, Lohner K, Henics T, Schütz GJ. Cationic amphipathic peptides accumulate sialylated proteins and lipids in the plasma membrane of eukaryotic host cells. *Biochim. Biophys. Acta* **2011**; 1808: 2581–2590.
25 Dube DH, Bertozzi CR. Glycans in cancer and inflammation — potential for therapeutics and diagnostics. *Nat. Rev. Drug Discov.* 2005; **4**: 477–488.
26 Li F, Ten Dam GB, Murugan S, Yamada S, Hashiguchi T, Mizumoto S, Oguri K, Okayama M, van Kuppevelt TH, Sugahara K. Involvement of highly sulfated chondroitin sulfate in the metastasis of the Lewis lung carcinoma cells. *J. Biol. Chem.* 2008; **283**: 34294–34304.
27 Fadnes B, Uhlin-Hansen L, Lindin I, Rekdal O. Small lytic peptides escape the inhibitory effect of heparan sulfate on the surface of cancer cells. *BMC Cancer* 2011; **11**: 116.
28 Gross S, Andrä J. Anticancer peptide NK-2 targets cell surface sulphated glycans rather than sialic acids. *Biol. Chem.* 2012; **393**: 817–827.
29 Goodrich L, Gerber H, Marti E, Antczak DF. Equine sarcoids. *Vet. Clin. North Am. Equine Pract.* 1998; **14**: 607–623, vii.
30 Yuan Z, Gault EA, Campo MS, Nasir L. Different contribution of bovine papillomavirus type 1 oncoproteins to the transformation of equine fibroblasts. *J. Gen. Virol.* 2011; **92**: 773–783.
31 Knottenbelt DC, Kelly DF. The diagnosis and treatment of periorbital sarcoid in the horse: 445 cases from 1974 to 1999. *Vet. Ophthalmol.* 2000; **3**: 169–191.
32 Drechsler S, Andrä J. Online monitoring of metabolism and morphology of peptide-treated neuroblastoma cancer cells and keratinocytes. *J. Bioenerget. Biomem.* 2011; **43**: 275–285.
33 Dempsey CE. The action of melittin on membranes. *Biochim. Biophys. Acta* 1990; **1031**: 143–161.
34 Andrä J, Leippe M. Candidacidal activity of shortened synthetic analogs of amoebapores and NK-lysin. *Med. Microbiol. Immunol.* 1999; **188**: 117–124.
35 Olak C, Muenter A, Andrä J, Brezesinski G. Interfacial properties and structural analysis of the antimicrobial peptide NK-2. *J. Pept. Sci.* 2008; **14**: 510–517.
36 Brandenburg K, Garidel P, Fukuoka S, Howe J, Koch MH, Gutsmann T, Andrä J. Molecular basis for endotoxin neutralization by amphipathic peptides derived from the alpha-helical cationic core-region of NK-lysin. *Biophys. Chem.* 2010; **150**: 80–87.
37 Beier M, Riebe R, Blankenstein P, Starick E, Bonzio A, Marquardt O. Establishment of a new bovine leukosis virus producing cell line. *J. Virol. Meth.* 2004; **121**: 230–246.
38 Andrä J, Koch MHJ, Bartels R, Brandenburg K. Biophysical characterization of the endotoxin inactivation by NK-2, an antimicrobial peptide derived from mammalian NK-lysin. *Antimicrob. Agents Chemother.* 2004; **48**: 1593–1599.
39 Whitmore L, Woollett B, Miles AJ, Janes RW, Wallace BA. The protein circular dichroism data bank, a Web-based site for access to circular dichroism spectroscopic data. *Structure* 2010; **18**: 1267–1269.
40 Whitmore L, Wallace BA. Protein secondary structure analyses from circular dichroism spectroscopy: methods and reference databases. *Biopolymers* 2008; **89**: 392–400.
41 Provencher SW. CONTIN: a general purpose constrained regularization program for inverting noisy linear algebraic and integral equations. *Comput. Phys. Commun.* 1982; **27**: 229–242.
42 van Stokkum IH, Spoelder HJ, Bloemendal M, van Grondelle R, Groen FC. Estimation of protein secondary structure and error analysis from circular dichroism spectra. *Anal. Biochem.* 1990; **191**: 110–118.
43 Banković J, Andrä J, Todorović N, Ana P-R, Đorđe M, Jannike K, Ruždijić S, Tanić N, Pešić M. The role of interaction between antimicrobial cationic peptide NK-2 and P-glycoprotein in overcoming multi-drug resistance in cancer. *Exp. Cell Res.* 2013; **319**: 1013–1027.
44 Liepinsh E, Andersson M, Ruysschaert J-M, Otting G. Saposin fold revealed by the NMR structure of NK-lysin. *Nat. Struct. Biol.* 1997; **4**: 793–795.
45 Warren P, Li L, Song W, Holle E, Wei Y, Wagner T, Yu X. *In vitro* targeted killing of prostate tumor cells by a synthetic amoebapore helix 3 peptide modified with two gamma-linked glutamate residues at the COOH terminus. *Cancer Res.* 2001; **61**: 6783–6787.

46 Kim S, Kim SS, Bang YJ, Kim SJ, Lee BJ. *In vitro* activities of native and designed peptide antibiotics against drug sensitive and resistant tumor cell lines. *Peptides* 2003; **24**: 945–953.
47 Boukamp P, Petrussevska RT, Breitkreutz D, Hornung J, Markham A, Fusenig NE. Normal keratinization in a spontaneously immortalized aneuploid human keratinocyte cell line. *J. Cell Biol.* 1988; **106**: 761–771.
48 Makovitzki A, Fink A, Shai Y. Suppression of human solid tumor growth in mice by intratumor and systemic inoculation of histidine-rich and pH-dependent host defense-like lytic peptides. *Cancer Res.* 2009; **69**: 3458–3463.
49 Gelhaus C, Jacobs T, Andrä J, Leippe M. The antimicrobial NK-2 peptide, the core region of mammalian NK-lysin, kills intraerythrocytic *Plasmodium falciparum*. *Antimicrob. Agents Chemother.* 2008; **52**: 1713–1720.
50 Gaspar D, Veiga AS, Sinthuvanich C, Schneider JP, Castanho MA. Anti-cancer peptide SVS-1: efficacy precedes membrane neutralization. *Biochemistry* 2012; **51**: 6263–6265.
51 Andrä J, Goldmann T, Ernst CM, Peschel A, Gutsmann T. Multiple peptide resistance factor (MprF)-mediated resistance of *Staphylococcus aureus* against antimicrobial peptides coincides with a modulated peptide interaction with artificial membranes comprising lysyl-phosphatidylglycerol. *J. Biol. Chem.* 2011; **286**: 18692–18700.

